

**GROUND CLUTTER SIGNAL ANALYSIS AND MODELING**

*V.M. KOSHEVOY **, *J.-P. HENRY ***,
*A.A. TANYGIN **, *S.T. TARABOUEV **, *V.V. RADIONOV **, *D. LE HELLARD ****

** State Polytechnic University, Odessa (Ukraine)*

*** Thomson-CSF-SDC, Direction Technique et Scientifique, 7 rue des Mathurins, 92223 Bagneux*

**** Laboratoire Radiocommunications, URA 834, Université de Rennes I, 35042 Rennes*

RESUME

Cet article présente un modèle phénoménologique de fouillis de sol qui prend en compte la corrélation existant entre les signaux rétrodiffusés par différentes parties du paysage. Ce modèle est basé sur l'utilisation de cartes topographiques ou numériques du terrain. Les propriétés de réflexion de la surface sont caractérisées par des paramètres qui dépendent de la rugosité du terrain; la rugosité à petite échelle étant décrite de manière statistique. Les variations dynamiques de la surface (dus aux turbulences atmosphériques) et les réflexions sur les objets artificiels sont aussi traitées dans ce modèle.

ABSTRACT

A ground clutter phenomenological model is presented. This model takes into account correlation between signals backscattered by different parts of surface. It is based on a land topographical or digital map data. Reflection properties of surface are characterized by parameters depending on terrain roughness degree. Small-scale roughness is described in a statistical sense. Dynamic variation of surface (e.g. due to atmospheric turbulence) and artificial objects reflections are also considered.

1. INTRODUCTION

Radar application of modern adaptive signal processing methods requires more adequate stochastic clutter models which include a subtle structure of correlation connections and spatial structure of clutter environment. Unfortunately, most of investigations on terrain and other clutter models are concerned with quantity relations establishing specific radar cross-section (RCS) for various surface types [1-3] and only a few of them consider spectral properties of reflected signals [1],[4],[5],[8]. Furthermore, there are no works in which the spectral and correlation properties in connection with correlation and inhomogeneity of different parts of surface were analyzed.

Reflected signal models based on the above mentioned approach enable us not only to simulate echo-signals more adequately but also to get a new knowledge on subtle structure of radar returns. Such models are more general as compared to those which should be obtained on the base of random numbers generating and should be used for a wide radar operating conditions, geographical and climatic conditions. Reflection properties of surfaces can be characterized by parameters depending on terrain roughness degree. The description of large scale roughness based on topographical or digital map with interpolating polynomial approximations are of most interest. Detailed behavior of roughness inherent in certain country can be described by means of a small-scale roughness only in a statistical sense. Another essential characteristic of a surface is its ability of shape variation under the influence of atmospheric turbulence. This influence is connected with dynamic behavior of scatterers (different parts of terrain) depending on weather, climatic conditions and other environmental factors that lead to variation of backscattered signal spectra. Obviously the models based on this approach are considerably more complex to construct and yield significant computational load when being realized. Therefore the problem of computational complexity is also considered in this paper.

2. CLUTTER ANALYSIS

Real echo-signals analysis allows to obtain more accurate models of clutter processes. To provide a research in this direction, results concerned with terrain spatial and statistical characteristics analysis have been obtained for different frequency bands, climatic conditions and terrain types. The main results of real data analysis for ground clutter are the following:

- strong spatial inhomogeneity of echoes in range and azimuth;
- dependence of backscattered signal spectra on the character of spatial and temporal nonstationarity of ground surface;
- strong variations of amplitude distribution for different resolution cells;
- existence of correlation dependence between signals reflected from different parts of terrain.

These results show that methods based on the generation of random numbers with prescribed statistical distribution and spectral properties cannot be used for ground clutter simulation: a great number of such generators would be necessary for terrain description, according to the variety of spatial and temporal properties of ground, in order to take into account possibility of correlation connections between different parts of terrain. From this point of view, using a phenomenological approach with allowance for phenomenon physics is much more preferable.

3. CLUTTER MODELING

3.1. Method of modeling

Land clutter modeling is based on topographical map analysis for the corresponding land site. At first, the topographical map is divided into resolution cells by plotting radial lines from radar position point. The angle between adjacent lines being equal to radar azimuthal resolution. Then circles are depicted with radius difference equal to range resolution interval. Obtained resolution cells are called first-order cells.



3.2. Earth surface altitudes interpolation and shadowing computation

Let us concern on earth surface relief construction for a certain resolution cell. This cell is partitioned into $K+1$ second-order cells of $\Delta x \times \Delta y$ surface size (Δy corresponds to some azimuth angle $\Delta \alpha$). In the first-order cell, the surface is described by the function $z(x,y)$ in rectangular coordinates. Hence the functions to be found are $z(x, y_0 + k\Delta y)$, $k=0, \pm 1, \dots, \pm K/2$, where y_0 is the ordinate of cell center. For each value of k , the abscissa x of intersections of $y_0 + k\Delta y$ lines with level lines taken from topographical map must be found. Denoting the abscissas of these n_k points as x_{ik} (value of x for each k), one can construct $K+1$ interpolating polynomials satisfying the condition

$$Z_k(x) = z(x, y_k), \quad k = 0, \pm 1, \dots, \pm K/2, \quad y_k = y_0 + k\Delta y.$$

Such polynomials could be constructed, for example, on the base of Lagrangian interpolating formula. To ensure description continuity between separate elements, adjacent elements are overlapping.

After the earth surface analytical description have been obtained, we can further partition the second-order cells into third-order elements of $\lambda/4$ size (λ wavelength).

The shadowing phenomenon is compute as follow: along a given azimuthal direction, all the second-order cells are analyzed in increasing order of range from the radar; the cells for which the elevation angle β is not smaller than the elevation angles of all preceding cells are considered as shadowed.

The remaining unshadowed cells, can be analyzed for a third-order elements shadowing, according to the same algorithm.

3.3. Complex reflection coefficients for angular - range elements

For each azimuthal direction α_p , one should construct sectors in elevation from β_{min} to β_{max} with step $\Delta \beta$. Then one forms, for each elevation sector β_{pj} , the array of complex reflection coefficients characterizing the earth surface reflection properties for the unshadowed second-order cells. These complex reflection coefficient should be defined as follows:

$$\sigma_{pjr} = \sigma_{pjr}^c \sigma_{pjr}^G c_{pjr} \cos \beta \quad (2)$$

where σ_{pjr}^G is the ground reflection coefficient, depending on the earth surface geometrical properties

$$\sigma_{pjr}^G = \frac{1}{M} \sum_{m=1}^M a_{pjr m} \exp(i4\pi d_{pjr m} / \lambda);$$

$d_{pjr m}$ = distance to element situated in p -th azimuthal direction, j -th elevation direction, r -th range second-order element and m -th third-order element;

$a_{pjr m}$ = shadowing coefficient, equal to 1 or 0;

M = number of 3rd order elements in the 2nd order element;

σ_{pjr}^c is the reflection coefficient allowing for cover nature (grass, cultivated land, snow, rocks, water,...), taking into account seasonal variations and radiation polarization (given by data-base); c_{pjr} is the area of the second-order cell getting into sector $\Delta \alpha, \Delta \beta$.

3.4. Reflected signal forming

Reflected radar signal depends on surface reflection properties (geometry and cover nature), signal shape and antenna pattern, and polarization. Let the transmitted signal be given as

$$S(t) = \sum_{n=1}^{N_F} \exp(i2\pi f_n t) \times \sum_{v=1}^{N_T} \sum_{n_v=1}^{N_V} u_0(t - (n_v - 1)T_v - (v - 1)N_{v-1}T - (n - 1)T_F) u_0(t) = \text{elementary pulse modulation law,}$$

- N_F = number of frequencies f_n in the train,
- N_V = number of pulses for single period value T_v ,
- T_F = repetition period of pulse trains for different carriers,
- N_T = number of different periods.

Then the reflected radar signal is [6]:

$$X(t) = \sum_{p=1}^{N_\alpha} \sum_{j=1}^{N_\beta} \sum_{r=R_{min}}^{R_{max}} G(\alpha_p - \alpha_0(t), \beta_j - \beta_0(t)) \times S(t - \Delta \tau_{pjr}) \sigma_{pjr}^{1/2} / d_{pjr}^2$$

where $\alpha_0(t) = \alpha_0 + \Omega_\alpha t$, $\beta_0(t) = \beta_0 + \Omega_\beta t$, $\Delta \tau_{pjr} = 2d_{pjr} / c$, Ω_α and Ω_β are the angular rates of steering and $G(\alpha, \beta)$ is the pattern of radar antenna.

Temporal samples of the signal formed from (4), with step by range resolution cell, are coupled in complex rectangular matrix, the columns of which correspond to range resolution cells within each period and the row corresponds to the period number. For non-periodic signal the columns x are of different sizes.

3.5. Small-scale roughness

The character of large-scale roughness is taken into account by the surface approximation polynomial construction. However, for reason of limited information amount extracted from topographical map, detailed behavior of roughness inherent in certain country can be described only in statistical sense. According to a current approach [1,4], normal distribution laws of altitude are used. Using large-scale variations, described by polynomial, as mean values of these distributions, one can describe deviations from the mean by a centered normal distribution law. The roughness character is then determined by the spatial covariance function of surface altitude:

$$\sigma_{\Delta z}^2 \rho_{\Delta z} = \sigma_{\Delta z}^2 \rho(x - x', y - y') \quad (5)$$

where $\sigma_{\Delta z}^2$ is the variance of surface altitude, $\rho_{\Delta z}$ the normalized spatial covariance function of surface altitude and (x,y) and (x',y') the coordinates of two arbitrary surface points. The function $\rho_{\Delta z}$ form and the variance depend on the terrain nature (soil character) or vegetation (grass, bushes, forest). The covariance functions may be set for each third-order element $\Delta x_j, \Delta y_j$ (or for combination of such elements), so that the sampling of ρ becomes:

$$\rho_{\Delta z nm} = \rho_{\Delta z}(n\Delta x_j, m\Delta y_j), \quad n, m = \overline{1, M}. \quad (6)$$

In a next step, random numbers corresponding to the small-scale surface roughness described in (5) are generated. The rough surface generation is achieved by a double linear transformation of an original vectors of independent normal random values. The random values $\Delta z(n x_j, m y_j)$ of surface altitudes may be obtained using a sectional filter [7]. A general requirement to a surface altitude covariance function is that its first derivative equals zero at $x = x', y = y'$. A function satisfying such requirement is [1]:

$$\rho_{\Delta z} = \sum_{i=1}^n a_i \exp(-(\frac{(x-x')^2}{l_x^2} + \frac{(y-y')^2}{l_y^2} + \frac{(x-x')(y-y')}{l_{xy}^2})) \quad (7)$$

where l_x and l_y are the spatial correlation lengths along X and Y axes and l_{xy} the mutual correlation radius.

A roughness character can be also described as a sum of a random component and a quasi-deterministic periodic function which can be expressed as:

$$\Delta z_\alpha(n\Delta x, m\Delta y) = \sum_{l=1}^s h_l \cos(\frac{l-n\Delta x_l}{A_x} + \frac{l-m\Delta y_l}{A_y}) \quad (8)$$

where h_l is the l -th harmonics amplitude of rolling surface and A_x and A_y are the spatial roughness periods along X and Y axes.

This periodic component (8) allows to describe rolling surface resulting from wind effects on vegetation cover and water surface. The value of spatial wave period and wave orientation can be controlled through A_x and A_y .

3.6. Surface dynamical properties under atmospheric turbulence

The water surface and vegetation cover change their geometry under influence of atmospheric turbulence such as wind, curls, etc. Surface geometry temporal variations can be obtained by introducing a temporal dependence in the covariance function used in the algorithm of rough surface generation (§3.5) such that

$$\Delta z_i(n\Delta x_i, m\Delta y_i, l\Delta t) = \frac{\Delta z(n\Delta x_i, m\Delta y_i) \cdot \chi(l\Delta t)}{\chi(\Delta t)} \quad (9)$$

where $\chi(l\Delta t)$ are samples of the random process. $\chi(l\Delta t)$ may be formed by a sectional filter [7]. The temporal covariance function $\rho(\tau)$ used can be

$$\rho(\tau) = \exp\left(-\frac{j\pi\sigma\Delta z}{\lambda} \cos \beta \frac{\tau^2}{l_\tau^2}\right) \quad (10)$$

where l_τ is the correlation radius of surface oscillations.

A nonstationary random temporal function can also be considered. If a quasi-deterministic periodic component is present in the surface roughness structure, one can allow for surface dynamic properties by introducing temporal dependencies directly into (8).

3.7. Reflections from artificial objects

Artificial objects such as buildings, chimneys, electric pylons, etc... yield perceptible exceeding of clutter returns level over background. Separately standing artificial objects or their couplings as distinct from terrain permit a strict functional description of their geometrical and physical properties. The strict solution of diffraction problem over an object give a rather complete and exact scattering model. However, realization of such model is available in extremely limited cases, so that various simplified representations appear [3]. Quasi-optical area approximations are more appropriate solutions when the object size considerably exceeds the wavelength; these methods allow to calculate a scattering diagram as a sum of contributions from separate parts of the object.

Actual objects can be modeled by bodies of simple forms. The complex object surface is partitioned into areas with known reflection properties, and separate scattering contributions are added [2,3]. For simplicity, the Kirchoff scattering model is used. In addition to this method, or instead of it, one can use multipoint models that describe object geometry as a set of points located on object surface $\lambda/4$ apart. With rectangular plates, one can approximate buildings, edifices, etc... Objects with smooth convex surfaces can be described by a multipoint model, however they allow a simpler description by one or more bright points.

If an object is connected with some Cartesian coordinate system (X, Y, Z) and its orientation in respect to radar is defined by angles θ and φ , where θ is measured from Z axis to radar direction, and φ - from positive X half-axis to radar ray incidence projection on (X, Y) plane, the range delay of the p -th bright point should be the function of this point coordinates θ and φ :

$$\tau_u = \tau_0 + \Delta\tau_u(\theta, \varphi) \quad (13)$$

where τ_0 is the time delay of the center of Cartesian coordinates connected with target, in respect to radar, and $\Delta\tau_u(\theta, \varphi)$ is the signal delay in respect to coordinate center. Radar cross-section of each complex object component also depends on angles θ and φ . Thus exploiting (13) one can represent the reflected signal as

$$X(t) = \frac{1}{(c\tau_0)^2} \sum_{u=1}^{N_u} \sigma_u^{1/2}(\theta, \varphi) \times S(t - \tau_0 - \Delta\tau(\theta, \varphi)) \cdot \exp(-j2\pi f\Delta\tau_u(\theta, \varphi)) \quad (14)$$

Under effect of atmospheric turbulence the object undergoes random perturbations which lead to random movement of complex target separate bright points and, as a result, to fluctuations of reflected signal.

Finally, the general expression for the signal reflected from

artificial objects and terrain background is:

$$X(t) = \sum_{p=1}^{N_\alpha} \sum_{j=1}^{N_\beta} G(\alpha_p - \alpha_0(t), \beta_j - \beta_0(t)) \times \quad (15)$$

$$\left(\sum_{r=R_{min}}^{R_{max}} S(t - \Delta\tau_{pjr}) \frac{\sigma_{pjr}^{1/2}}{d_{pjr}^2} + \sum_{u=1}^M S(t - \Delta\tau_{pju}) \frac{\sigma_{pju}^{1/2}}{d_{pju}^2} \exp(-j \frac{2\pi c}{\lambda} \Delta\tau_{pju}) \right)$$

where M is the total number of bright points of artificial objects in the observable area, N_l is the number of bright points in the l -th object, and L is the number of artificial objects.

3.8. Some ways to improve computational efficiency

The above algorithms of terrain returns simulation have wide possibilities to describe the covers of very various nature; however their computational load is quite high in some cases and some ways of computational complexity reduction may be used.

First of all, Lagrangian interpolating polynomials have high polynomial order. From the standpoint of computational load and memory requirements, the use of polynomials with predetermined order - such as Kolmogorov-Gabor polynomials - may be more preferable. Coefficients of the polynomial can be obtained by Least-squares surface interpolation method.

Another drawback of computational nature appears when replacing surface by multipoint model. The number of points involved to summation in (2) may turn out to be very large. Since small-scale roughness for different second-order elements might have similar character to a considerable extent, surface can be approximated by a set of equal areas arranged in a certain way to reproduce large-scale character of country relief. So, we should come to the so-called facet model of surface. In our case the second-order elements could be replaced by corresponding flat facets oriented in accordance with surface samples spacing at points which are in keeping with variables arrangement network for the second-order elements. Flat plates of appropriate size can be used as such facets. Since a plane is defined by three points in space, to approximate each second-order element containing four points of surface samples, one can use two flat surfaces as triangular plates passing through each three points of the surface.

As real surfaces contain roughness of some kind, we should obtain more adequate model by drawing through each three points a rough facet instead of a flat one. For this rough facet the reflection coefficient is determined by [1]:

$$G(\theta, \varphi) = \frac{\sigma_m}{\sqrt{2\sigma_n((\rho''_n)_x(\rho''_n)_y - (\rho''_n)_{xy})^2}} \exp\left\{-\frac{tg^2\theta \cos^2\varphi}{4\pi(\rho''_n)_x}\right\} \times \exp\left\{-\frac{tg^2\theta \left[\sin\varphi - \cos\varphi \frac{(\rho''_n)_{xy}}{(\rho''_n)_x}\right]^2}{4\sigma_n^2} \frac{(\rho''_n)_x^2}{(\rho''_n)_x(\rho''_n)_y - (\rho''_n)_{xy}^2}\right\}$$

where $(\rho''_n)_x$, $(\rho''_n)_y$ and $(\rho''_n)_{xy}$ are the second derivatives of surface covariance function on each variable and the mixed one at point $x=0, y=0$.

Formula (16) has been derived without shadowing consideration and may cause errors at large angles. We can use the numerical method stated in §3.3 to obtain rough facet reflection coefficient with shadowing effect consideration. In this case one should generate random realizations of the rough facet - with given covariance function and roughness variance - and calculate the reflection coefficients for a discrete set of angles θ and φ . The random realizations are then averaged to obtained a reflection diagram. Continuous diagrams over angles θ and φ are obtained through interpolation by smoothing functions. The results show that diagrams main lobe widen as roughness meansquare height grows. A diagram is recorded as a set of coefficients, which allows to calculate, using interpolating functions, the reflection coefficient for a given facet with angles θ and φ . Thus the computational load is significantly reduced.

4. RESULTS

Some examples of ground clutter signal modeled are presented in this chapter.

The record of real signal reflected by a chimney is presented in Fig.1, for different values of pulse repetition periods (stopped antenna). Fig.2 corresponds to modeled signal. One could get new information about reflections using adopted model, for example to investigate chimney signal fluctuations in time due to the wind influence; this case is illustrated by Fig.3. The mean square value of deviation of the highest point of the chimney is 1 cm ($\lambda=3\text{cm}$).

Fig.4 corresponds to the modeling of reflections from some hilly locality in the case of rotating antenna. The data is presented on a range-azimuth plane.

The real signal record for reflection from forest is presented in Fig.5 (stopped antenna). Signal fluctuations due to the wind can be seen on this figure. The corresponding modeled signal is drawn in Fig.6; one can see a good agreement with the real data.

5. CONCLUSION

We have performed a search for new models of echo signals from earth and other radiophysical objects. Provided analysis of spatial-temporal distributions show that terrain reflections are extremely inhomogeneous in time and azimuth domains. In a general case terrain can be represented as a total combination of areas with comparatively uniform clutter and a set of well-separated dominant scatterers.

Surface phenomenological models are developed which allow for subtle structure of reflected signals, particularly the possible correlation of reflections from the different surface parts with their connections to topographical map. Models of artificial objects have also been derived.

ACKNOWLEDGMENT

The authors gratefully acknowledge the "Direction des Recherches, Etudes et Techniques" (DRET) of the French "Délégation Générale de l'Armement" (DGA), who supported the work presented in this paper.

REFERENCES

- [1] Zubkovich S., *Statistical characteristics of reflections from ground.*- Moscow: Sov.radio, 1970 - 224 p.
- [2] Ruck G.T., *Radar cross section handbook.*- N.Y.: Plenum Press, 1970.
- [3] Crisgin E.J.W., Siegel K.M., *Methods of radar cross section analysis.*- N.Y.: Academic Press, 1968.
- [4] *Earth investigations with radar.* Ed. U.Melnik - Moscow: Sov. radio, 1980 - 262 p.
- [5] Dubov A., Bykov A., Marunich S., *Turbulence in vegetation* - Leningrad: Hydrometeoizdat, 1978 - 256 p.
- [6] Abramovich Yu.I., Koshevoy V.M., Lavrinenko V.P., 'Ambiguity function of reflections from extended targets', *Radiotekhnika i elektronika*, 1977, v.22, N10, p.2109 - 2115.
- [7] Koshevoy V.M., 'Recursive algorithms synthesis for optimal signal processing', *Izvestiya vuzov. Radioelektronika*, 1985, v.28, N11, p.14-15.
- [8] Kulyomin G.P., Razskazovsky V.B., *Microwave radiowaves backscattering by the earth surface on low grazing angles.*- Kiev: Naukova Dumka, 1987.

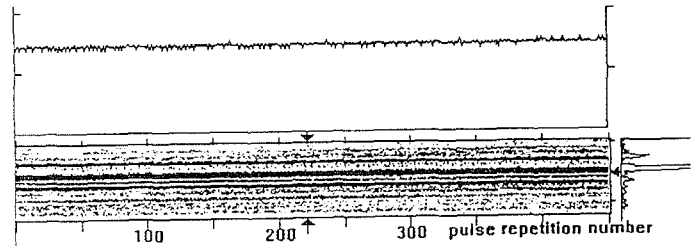


Figure 1 - Record of real signal reflected from chimney

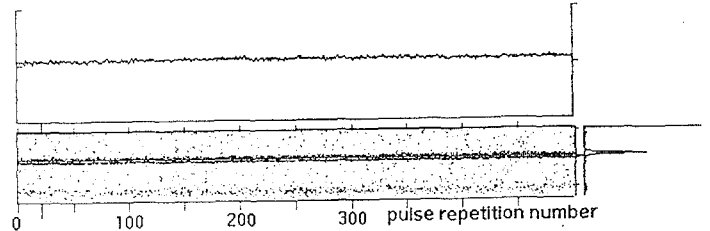


Figure 2 - Simulated chimney reflections.



Figure 3 - Simulated chimney reflections fluctuating due to wind

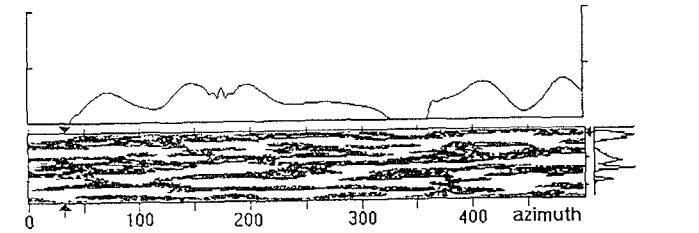


Figure 4 - Simulated reflection from hilled area (Range-Azimuth plane)

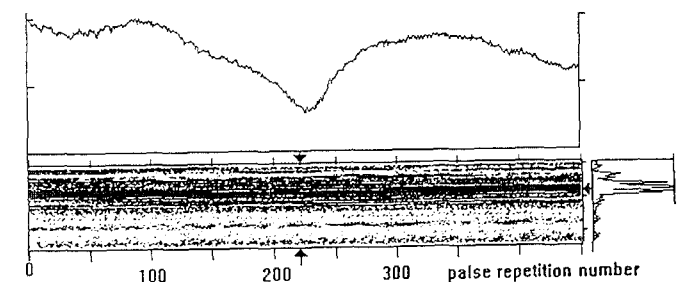


Figure 5 - Record of real signal reflected from forest.

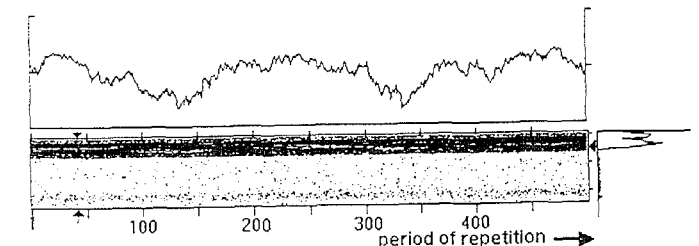


Figure 6 - Simulated forest reflections.